Progress in Biomaterials (2020) 9:35–44
https://doi.org/10.1007/s40204-020-00130-7

ORIGINAL RESEARCH

Fabrication of a novel hydroxyapatite/polyether ether ketone surface nanocomposite via friction stir processing for orthopedic and dental applications

Davood Almasi[1] · Woei Jye Lau[2] · Sajad Rasaee[3] · Roohollah Sharifi[1] · Hamid Reza Mozaffari[4,5]

Received: 29 February 2020 / Accepted: 26 April 2020 / Published online: 3 May 2020

Abstract
There is increasing interest in the use of polyether ether ketone (PEEK) for orthopedic and dental implant applications due to its elastic modulus (close to that of bone), biocompatibility and radiolucent properties. However, PEEK is still categorized as bioinert owing to its low integration with surrounding tissues. Methods such as depositing hydroxyapatite (HA) onto the PEEK surface could increase its bioactivity. However, depositing HA without damaging the PEEK substrate is still required further investigation. Friction stir processing is a solid-state processing method that is widely used for composite substrate fabrication. In this study, a pinless tool was used to fabricate a HA/PEEK surface nanocomposite for orthopedic and dental applications. Microscopical images of the modified substrate confirmed homogenous distribution of the HA on the surface of the PEEK. The resultant HA/PEEK surface nanocomposites demonstrated improved surface hydrophilicity coupled with better apatite formation capacity (as shown in the simulated body fluid) in comparison to the pristine PEEK, making the newly developed material more suitable for biomedical application. This surface deposition method that is carried out at low temperature would not damage the PEEK substrate and thus could be a good alternative for existing commercial methods for PEEK surface modification.

Keywords PEEK · Hydroxyapatite · FSP · Nanocomposite · Pin-less tool · Bioactivity

Introduction

Polyether ether ketone (PEEK) is a very interesting material for orthopedic and dental applications owing to its chemical resistance, elastic modulus that is close to the bone elastic modulus and radiolucency (Almasi et al. 2016). However, low bioactivity of PEEK is the main problem that limits its biomedical application. In order to enhance the bioactivity of implants, bioactive material—hydroxyapatite (HA) with the ratio of calcium to phosphorus similar to the natural bone has been previously considered (Shen et al. 2014). Fabrication of composites using HA additive is one of the strategies to increase the bioactivity of the PEEK, making it as bioactive implant material (Aravind and Sangeetha 2015; Pan et al. 2013).

Melt mixing and injection molding are the common methods to produce HA/PEEK composites (Bakar et al. 2003). However, these methods are always associated with nanoparticles agglomeration during nanoparticle reinforcement process (Roeder et al. 2008; Wang et al. 2010, 2011). Currently, surface modification of PEEK using plasma spraying is the most effective method. However, plasma spraying of HA is required to be carried out at a high temperature and because of this, it will not suitable for low-melting point PEEK. Although the low temperature has been previously applied, a strong adhesion between the PEEK substrate and HA layer is hard to achieve (Filiaggi et al. 1991; Rabiei and

✉ Sajad Rasaee
rasaee@kut.ac.ir

1 Department of Endodontic, School of Dentistry, Kermanshah University of Medical Sciences, Kermanshah, Iran

2 School of Chemical and Energy Engineering, University Teknologi Malaysia, 81310 Skudai, Johor, Malaysia

3 Department of Mechanical Engineering, Faculty of Energy, Kermanshah University of Technology, Kermanshah, Iran

4 Department of Oral and Maxillofacial Medicine, School of Dentistry, Kermanshah University of Medical Sciences, Kermanshah, Iran

5 Medical Biology Research Center, Kermanshah University of Medical Sciences, Kermanshah, Iran

Sandukas 2013; Radin and Ducheyne 1992). In order to address the drawbacks, friction stir processing (FSP),a solid phase processing technique, can be employed to modify the surface of PEEK (Ahmed et al. 2018). For this method, the additives are homogenously mixed with the substrate material without the need for melting the substrate.

FSP method has been widely used for fabricating substrates made of magnesium (Morishige et al. 2008) and titanium (Farnoush et al. 2013b). Although some thermoplastic polymers have been treated using this method (Gan et al. 2010; Prasad and Raghava 2012), some concerns relating to macromolecular chain breaking are raised as a result of tool pin rotation (Gan et al. 2010). Squeeze-out of plasticized or semi-molten polymer is also the main concern regarding the friction stir welding (FSW) or FSP of the polymeric materials (Paoletti et al. 2016). In view of this, pinless tool is the most appropriate technique to prevent squeeze out of material (Costa et al. 2014).

FSP has been used widely to fabricate surface nanocomposites with enhanced mechanical properties (Farnoush et al. 2013a), increased bioactivity (Ratna Sunil et al. 2014a) and reduced degradation rate (Ratna Sunil et al. 2014b). HA is one of the additives which has been widely used for composite fabrication via FSP. Using HA as an additive for the fabrication of magnesium-based composite via FSP could decrease degradation rate of magnesium/HA surface composite (Ratna Sunil et al. 2014b), improve corrosion resistance as well as increase hydrophilicity and cell viability (Ratna Sunil et al. 2014a). HA-modified titanium composite fabricated via FSP had increased the bonding strength of the deposited HA by electrophoretic on the titanium substrate, as well as increased its corrosion resistance property (Farnoush et al. 2013b). It is also found that the HA-modified titanium composite tended to exhibit higher micro-hardness and corrosion resistance properties than that of bare titanium substrate (Farnoush et al. 2013a).

In this study, FSP method based on a pinless tool was employed to fabricate a HA/PEEK surface nanocomposite for biomedical applications. The deposition and distribution of the HA nanoparticles on the surface of PEEK substrate were investigated using a scanning electron microscope (SEM) coupled with energy dispersive X-ray (EDX) spectroscope. X-ray diffraction (XRD) and water contact angle characterizations were also performed to confirm the crystallinity of the deposited HA and hydrophilicity properties of the surface nanocomposite, respectively. In vitro apatite formation of the samples was evaluated to probe the bioactivity properties of the newly fabricated HA/PEEK surface nanocomposite.

Experimental

Sample preparation

PEEK substrate (1.9-cm in diameter) used in this experiment was obtained from Optima® Invibio. The surface of the PEEK substrate was grounded by 220-grit silicon carbide paper before it was subjected to ultrasonic cleaning in acetone. The rough surface of the PEEK discs was covered by HA and ethanol (to prevent the separation of the HA powder from the PEEK substrate) by the wind of the rotating tool. Pinless tool with the flat surface of 1.9cmin diameter was used to fabricate surface nanocomposite. Figure 1 illustrates the schematic of the HA/PEEK surface nanocomposites fabrication via FSP method. Preliminary experiment was conducted to find the optimum fabrication conditions. At the low rotation speed, the created heat was insufficient to heat the PEEK surface. At high rotation speed coupled with prolonged contact time between the tool and samples, the PEEK surface was damaged. Low thermal conductivity of the PEEK sample could keep the created heat on the sample surface, partially increasing the temperature. The preliminary experiment found that the appropriate contact time and rotation speed for HA/PEEK surface nanocomposite fabrication should be maintained at 2 s and655 rpm, respectively. The modified samples were then put in the ultrasonic bath to remove the undeposited HA.

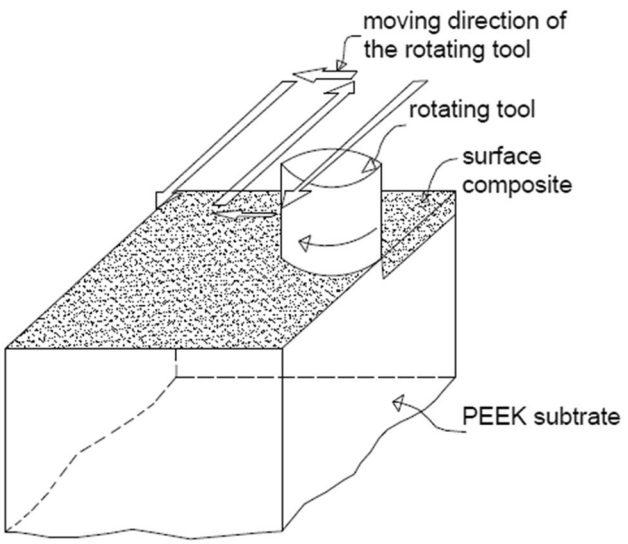

Fig. 1 Schematic HA/PEEK surface nanocomposite fabrication through FSP

Sample characterisation

Surface morphology of the resultant surface nanocomposites was examined using a scanning electron microscope (SEM) (MIRA3 TESCAN CZECH). Energy dispersive X-ray (EDX) spectroscope was used to analyze the chemical composition of the HA/PEEK surface nanocomposite. Chemical composition and crystallinity (X_c) of deposited HA meanwhile were analysed using XRD diffraction with a Cu X-ray tube (Siemens D5000 Diffractometer). The analysis was carried out at 40 kV and 30 mA, with data collected in the range of 20°–80° with the step size of 0.05°. The degree of crystallinity (X_C) of the HA powder was calculated using Eq. (1) (Landi et al. 2000):

$$\beta_{002}\sqrt[3]{X_C} = K, \tag{1}$$

where K is the constant equal to 0.24 for HA and β_{002} is the full width at half maximum (FWHM) of the (002) plane (Landi et al. 2000).

An atomic force microscope (AFM) (SPA-300 HV, Seiko) using Olympus micro cantilever (OMCL-TR400PSA-3) was used to analyze the surface roughness of the samples. The AFM scanning was run in a force curve mode over a scan size of 5 µm × 5 µm. Thirty lines, each with a length of 5 µm was used to calculate the average arithmetic mean surface roughness (R_a). Contact angle goniometer (OCA 15plus, DataPhysics) was used for the measurement. The ASTM D7334-08 standard was used for doing the test, where deionised water was used as the liquid and the chosen drop size was0.5 ± 0.1 µL. For each sample, 10 points were randomly chosen from the sample surface and measurement was taken within 30 s after the drop to yield the average result. If the contact angle on the two edges were deviated by > 2°, such values were eliminated.

The progressive scratch test was carried out using nano-scratch test equipment (Micro Materials Limited) with the scanning length of 600 µm and velocity of 2 µm/s. The normal load was not applied on the stylus for the first 60 µm. The normal load was set to increase linearly from 0 to 500 mN at a loading rate of 2 mN/s, between 60 and 560 µm and it remained constant at the last 40 µm. Conical spherical Rockwell stylus was used for conducting the test. Formation of apatite layer from simulated body fluid (SBF) is a widely used method which enables prediction of in vivo bone-bonding tendency of the material (Kokubo 1998; Kokubo and Takadama 2006). For the apatite formation test, the samples were immersed in SBF solution provided by Nik Ceram Razi Corporation (Iran) and kept in a water bath at a fixed temperature (37° C). The surface ratio of the sample to the volume of the SBF solution had a value almost equal to 0.02 cm^{-1} (Strnad et al. 2000). SEM analysis was used to examine the apatite formation on the surface of HA/PEEK surface nanocomposite after 1, 3 and 7-day immersion in the SBF. The data of this study were analyzed by SPSS Statistics 22 (IBM, USA) using one-way analysis of variance (ANOVA) and Tukey's test followed by post hoc least significant difference (LSD), with a significance level set at $p < 0.05$.

Results

Surface morphology of the treated layer

Figures 2a, b show the surface morphology of PEEK/HA surface nanocomposite at different magnification. Using the optimum fabrication conditions, the HA nanoparticles distributed homogenously at the surface of the PEEK/HA surface nanocomposite and appears in the range of nanometer without agglomeration. Figure 2c shows the surface morphology of bare PEEK before surface modification. Figure 2d, e compares the EDX surface mapping of the PEEK/HA nanocomposites with the bare PEEK. The detection of calcium element on the PEEK/HA surface nanocomposite confirms the existence of HA nanoparticles on the PEEK surface.

XRD analysis

Figure 3 shows the XRD spectra of the HA powder and-PEEK with and without HA modification. For the HA powder, the peaks that correspond to the crystalline phase are compared with International Center for Diffraction Data (ICDD 9-432) and labeled using their related crystallographic planes (Rabiei and Sandukas 2013). The XRD spectrum of the PEEK exhibits three high-intensity peaks, i.e., 21°, 22.6°, and 28.7° and can be attributed to the (113), (200), and (213) of crystallographic planes, respectively. The results are consistent with the findings reported in the work of Zhang et al. (2006). For the PEEK/HA surface nanocomposite samples, the XRD spectrum indicates a slight intensity of peaks belonging to the (002) and (211) crystallographic planes of HA. These two peaks confirm the existence of crystalline HA nanoparticles in the treated layer.

Crystallinity property of the coated HA is one of the most important parameters which affects the mechanical properties and solubility property of the coating layer and subsequently affect stimulation of bone growth around the implant and implant fixation (Chou et al. 1999; Xue et al. 2004). The average calculated X_c for two surface nanocomposites samples was 68.32 ± 1.76% which has the same value as the HA powder. This result confirms that FSP surface modification method that conducted at its low temperature does not affect the crystallinity of the deposited HA.

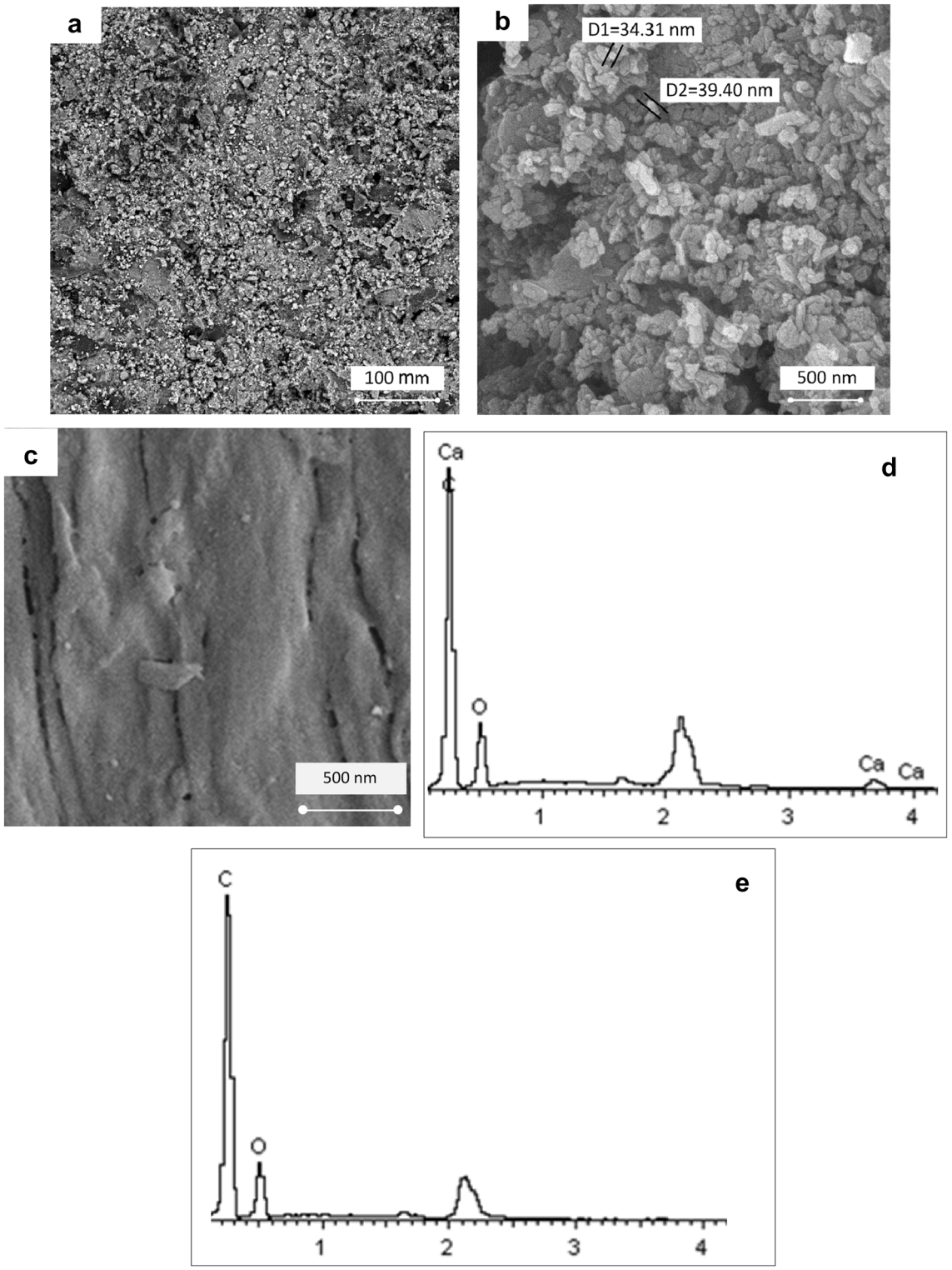

Fig. 2 **a**, **b** SEM surface images of PEEK/HA nanocomposite with different magnifications, **c** SEM surface image of PEEK, **d**, **e** EDX results of PEEK/HA nanocomposite and bare PEEK

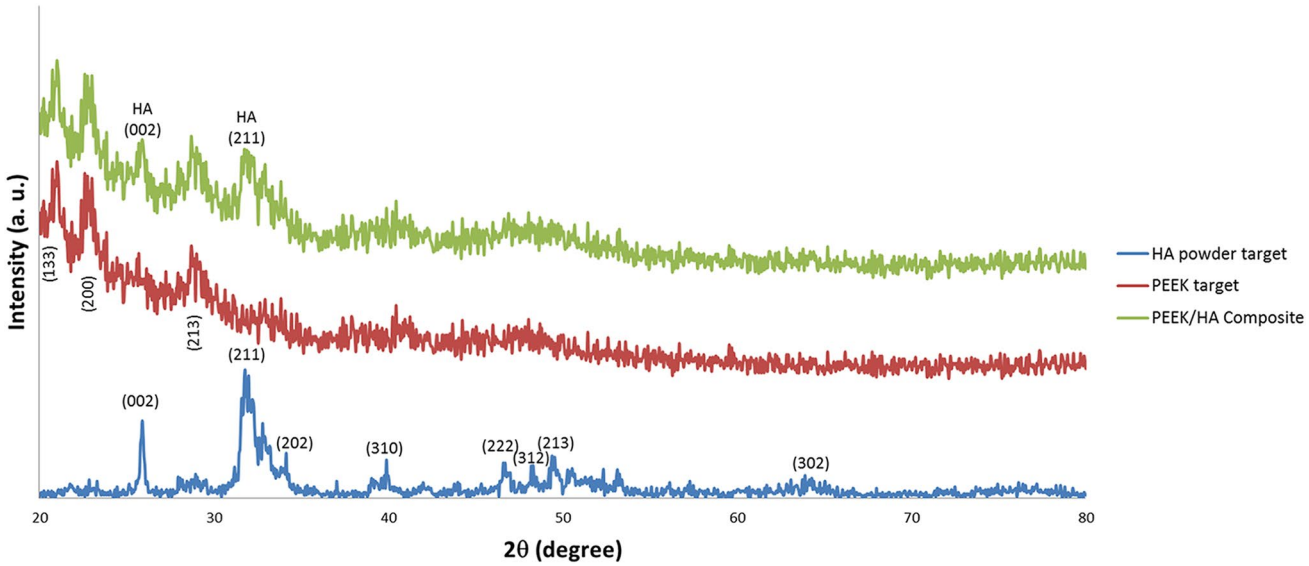

Fig. 3 XRD spectra of HA, PEEK, and PEEK/HA surface nanocomposite

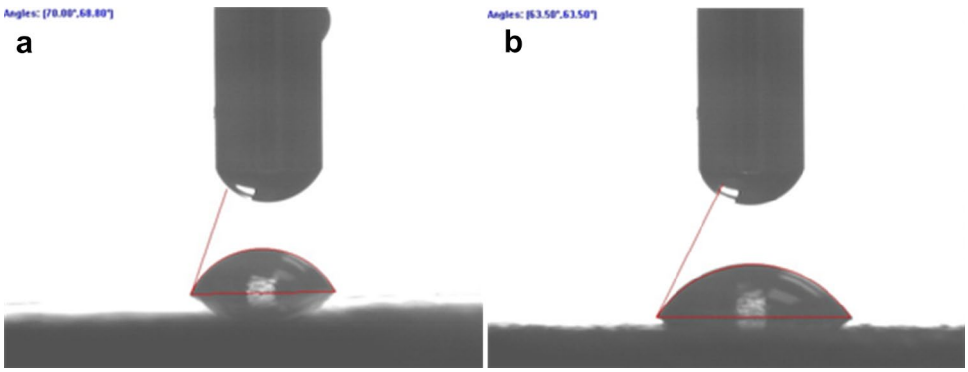

Fig. 4 Images of water droplet on the surfaces of **a** PEEK and **b** HA/PEEK nanocomposites

Water contact angle

Figure 4 shows the single water droplet on the surface of the PEEK sample before and after HA modification. Compared to the pristine PEEK, the water contact angle of the HA-modified PEEK was reduced significantly from$71.6° \pm 3.8°$ to $63.2° \pm 4.6°$, indicating the improvement in surface hydrophilicity upon HA modification ($p < 0.05$).

Scratch test results

Figure 5a, b present the SEM surface images of the HA/PEEK surface nanocomposite. Whenever the applied shear stress using the stylus overcomes the ultimate shear strength of the coating layer material, the coating layer undergoes the plastic deformation and the material slip on each other and macro-chip will be formed. The accumulation of the plastically deformed material made the macro-chip getting bigger during the scratch test. The formed macro-chip placed under the stylus and pushes the stylus up during the scratch test. Considering the soft property of the substrate used in this study, the macro-chip stuck to the stylus continued the removing of the material even after reaching the substrate. This phenomenon occurs due to the reduction of stylus penetration depth at the end of the scratch track because of macro-chip accumulation under the stylus (Fig. 5a). At the edges of the scratch on the treated layer, some cracks are visible due to the compression load which was applied by stylus during the test (Fig. 5b). There is no macro-chip material ahead or under the stylus for the brittle coating layer and the only factor which affects the penetration depth is the normal load (Liu et al. 2009; Xu et al. 2014). However, the macro-chip was reported for the soft coating layer (Barletta et al. 2011).

Figure 5c indicates the penetration depth and normal load against the scratch distance of the surface nanocomposite. The penetration depth of the stylus ought to increase with increasing normal load. However, the

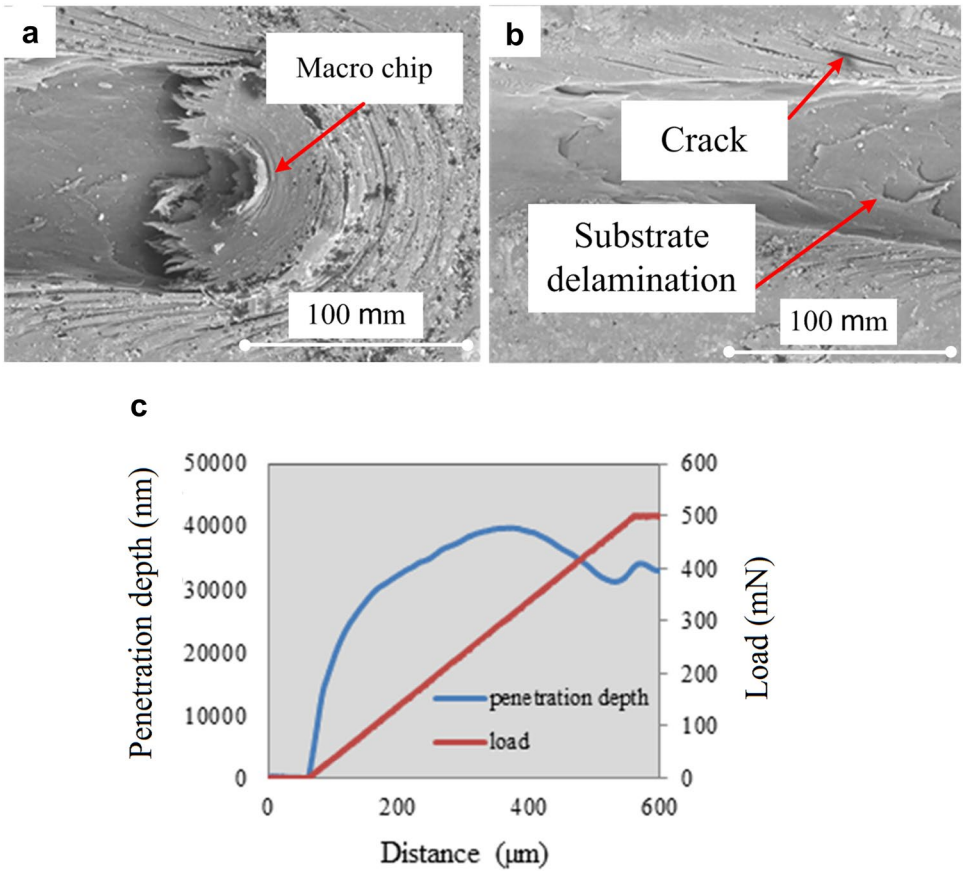

Figs. 5 **a**, **b** Scratch image of the surface nanocomposite through SEM, **c** penetration depth versus scratch distance

accumulation of the detached coating and substrate material ahead and under the stylus (macro-chip) pushes the stylus up, affecting the penetration depth. The push-up force by the formed macro-chip under the stylus (Fig. 5a) tended to overcome increasing normal load due to the reduction of stylus penetration depth at the last part of the scratch distance.

AFM results

Figure 6 presents the 3D AFM surface images of the PEEK and HA/PEEK surface nanocomposite. The surface of then a nocomposite becomes rougher in comparison to the bare PEEK in which the R_a value increases from 20.3 to 34 nm ($p < 0.05$). However, due to the soft property of polymer composites, the HA/PEEK surface nanocomposite has the feasibility to be polished or implying subsequent heat

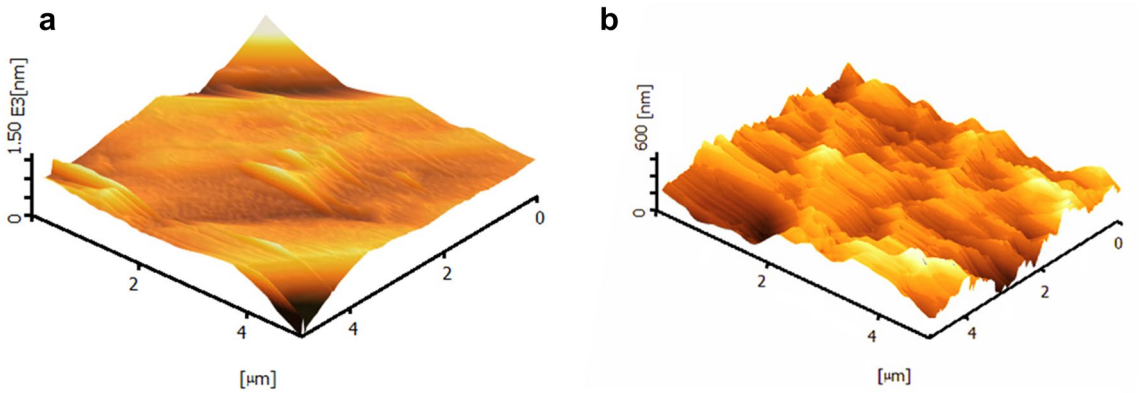

Fig. 6 AFM 3D height image of **a** PEEK and **b** HA/PEEK surface naocomposite

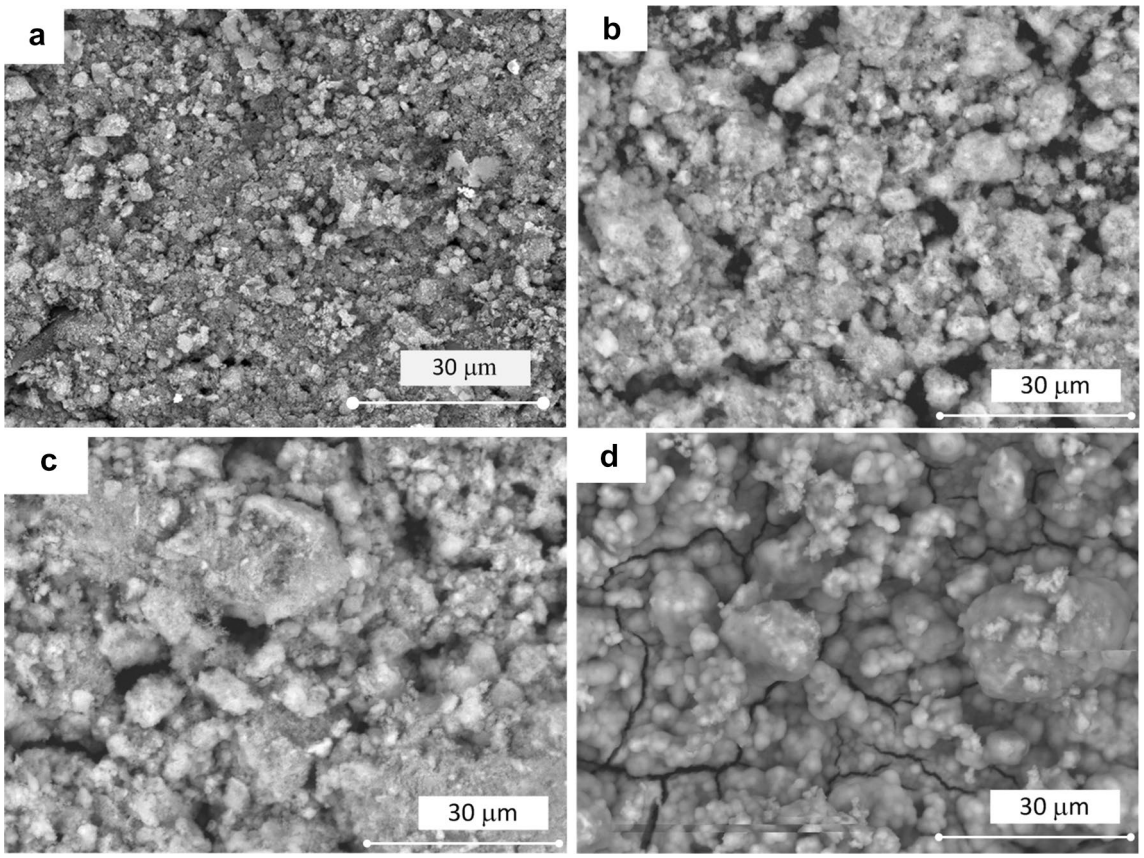

Fig. 7 SEM image of the apatite formation on the surface of HA/PEEK nanocomposite **a** before and after **b** 1 day; **c** 3 days and **d** 7 days immersion in SBF solution

Table 1 Elements weight percentage of the material surface after immersing in SBF solution for different days

Element (weight %)	Before immersion	1st day	3rd day	7th day
Carbon	50.31	34.15	17.46	0
Oxygen	28.42	30.58	31.71	37.74
Phosphorus	6.13	11.39	15.39	18.74
Calcium	15.14	23.88	35.45	43.52

treatment to catch the desire surface roughness. This unique property of the surface nanocomposite can be considered advantageous of this fabrication method.

In vitro apatite formation

Figure 7 shows the SEM images of the HA/PEEK surface nanocomposite and bare PEEK samples after immersion in the SBF for up to 7 days. Formed bone-like apatite on the surface of the HA/PEEK surface nanocomposites suggested that the bioactivity of the HA/PEEK surface nanocomposite is higher than the bare PEEK. After 7 days, the whole surface of the surface nanocomposite sample was covered by spherical apatite layer. Table 1 presents the weight percentage of the elements at the surface of the specimens that were measured via EDX analysis. The results confirm the complete coverage of the apatite after 7th day of immersion. The weight percentage of the carbon was zero after 7-day immersion in the SBF solution, confirming the formed apatite layer completely covered the surface of the HA/PEEK surface nanocomposite. Apatite formation on the surface of the bare PEEK samples was not observed after 2-week immersion in the SBF. The results reveal that the HA/PEEK surface nanocomposites exhibited better apatite formation ability, showing better interaction with the surrounding bone in the body.

Discussion

There are several conventional methods to deposit HA onto the PEEK surface. These include plasma spraying (Ha et al. 1994), cold spraying (Lee et al. 2013), aerosol deposition (Hahn et al. 2013) and vacuum plasma spraying (Ha et al. 1997). However, these conventional methods

tend to cause damage to PEEK surface due to the use of high temperature during deposition or crystallization process (Ha et al. 1994; Rabiei and Sandukas 2013). The fabrication method as proposed in this work is very simple and requires no special equipment. Very good adhesion layer was obtained on the new surface nanocomposite and no delamination of the surface nanocomposite layer from the substrate was observed. Using this fabrication method, the crystallinity of the HA deposition will not be affected as it does not involve high temperature. Furthermore, it does not need any subsequent crystallization process to increase HA crystallinity.

Mixing PEEK with bioactive materials such as HA via compounding and injection molding process and fabrication of nanocomposite is another approach to increase the bioactivity of PEEK (Roeder et al. 2008). However, agglomeration of the HA nanoparticles tends to be very severe especially when excessive HA is used in the nanocomposite. While the hydroxyapatite size is one of the main factors which directly affect the promotion of cell attachment, cell growth, cell apoptosis inhibition, nano-sized HA demonstrates better bioactive property in comparison to micro-sized HA (Huang et al. 2004; Müller et al. 2014; Shi et al. 2009). Implants made of PEEK nanocomposites have a number of advantages such as increased bioactivity and better mechanical properties (Wang et al. 2014; Wu et al. 2012). Other studies also reported a tendency of nanoparticles to agglomerate during nanoparticle-reinforced thermoplastics fabrication (Roeder et al. 2008; Wang et al. 2010, 2011). In FSP fabrication method, the additive and substrate are mixing very well due to its high tool rotation speed. This is one of the significant advantages of this method in comparison to the existing fabrication methods.

The surface roughness of the surface nanocomposites is reported to be higher compared to the bare PEEK. As shown, the micro and nano-size topographical profile (roughness) are visible respectively in Fig. 2a, b. Micro-sized topographical profile enhances osteoconduction and osteoinduction, causing better bone-to-implant contact (Stanford 2008). Nano-sized topographical profile on implant surface enhances the adsorption of proteins, adhesion of osteoblastic and osseointegration enhancement (Alla et al. 2011; Mendonça et al. 2008). Thus, HA/PEEK surface nanocomposite can be an ideal choice with providing micro and nano-size topographical profile at the surface.

Water contact angle data indicate that the changes in chemical structure and roughness of the PEEK via this method decrease the water contact angle of PEEK from $71.6° \pm 3.8°$ to $63.2° \pm 4.6°$. For biomedical application, the lower water contact angle leads to better cell attachment (Arima and Iwata 2007).

Conclusion

This study reported a method to deposit HA onto the PEEK surface via FSP method. This technique does not involve high temperature during the fabrication process, and thus would not affect the crystallinity of the deposited HA. EDX analysis confirmed the HA deposition while SEM surface images showed fine dispersion of HA nanoparticles in the surface nanocomposite in the range of nanometer. Well dispersion of the nanoparticles as a result of well-mixing polymer matrix and additive was the positive outcome that could be obtained from this fabrication method. XRD results confirmed the crystallinity property of the deposited HA. Therefore, there was no need to subject to subsequent crystallisation to increase the crystallinity of the deposited HA. The water contact angle of the surface nanocomposite was reduced in comparison to the bare PEEK which can be a sign of bioactivity enhancement. Bone-like hydroxyapatite formation on the surface of the HA/PEEK surface nanocomposite in the SBF solution confirmed PEEK bioactivity enhancement via our new surface modification method. The nano-scratch study confirmed an adhesive attachment of the PEEK/HA surface nanocomposite. There was no delamination between the coating layer and substrate with penetration of stylus. Due to above-mentioned properties, deposition of HA on the surface of the PEEK using FSP method could be potentially considered as a replacement of existing deposition methods.

Future work

In this study, FSP was used for the first time to fabricate PEEK/HA surface nanocomposite. In vitro and in vivo studies are still required to confirm the feasibility of the fabricated HA/PEEK surface nanocomposite for orthopaedic and dental implant application. The impacts of the subsequent heat treatment and the fabrication parameters that affect the surface morphology and bioactivity of the surface are worthy of further investigation.

Acknowledgements This article was a result of a study conducted at Kermanshah University of Medical Sciences in Kermanshah, Iran.

Compliance with ethical standards

Conflict of interest The author declares that there are no conflicts of interest regarding the publication of this paper.

Ethical statement This research was evaluated in accordance with the ethical principles by Kermanshah University of Medical Science at 2018.07.31 and approved with the approval ID: IR.KUMS.RES.1397.285. The research was found to be in accordance with the

ethical principles and the national norms and standards for conducting Medical Research in Iran. This research was not involving human participants and animals.

References

Ahmed H, Van Tooren M, Justice J, Harik R, Kidane A, Reynolds AP (2018) Investigation and development of friction stir welding process for unreinforced polyphenylene sulfide and reinforced polyetheretherketone. J Thermoplast Compos Mater. https://doi.org/10.1177/0892705718785676

Alla RK, Ginjupalli K, Upadhya N, Shammas M, Ravi RK, Sekhar R (2011) Surface roughness of implants: a review. Trends Biomater Artif Organs 25:112–118

Almasi D, Iqbal N, Sadeghi M, Sudin I, Abdul Kadir MR, Kamarul T (2016) Preparation methods for improving PEEK's bioactivity for orthopedic and dental application: a review. Int J Biomater 2016:12. https://doi.org/10.1155/2016/8202653

Aravind K, Sangeetha D (2015) Characterization and in vitro studies of sulfonated polyether ether ketone/polyether sulfone/nano hydroxyapatite composite. Int J Polym Mater Polym Biomater 64:220–227. https://doi.org/10.1080/00914037.2014.936594

Arima Y, Iwata H (2007) Effect of wettability and surface functional groups on protein adsorption and cell adhesion using well-defined mixed self-assembled monolayers. Biomaterials 28:3074–3082. https://doi.org/10.1016/j.biomaterials.2007.03.013

Bakar MA, Cheang P, Khor K (2003) Tensile properties and microstructural analysis of spheroidized hydroxyapatite–poly (etheretherketone) biocomposites. Mater Sci Eng A 345:55–63

Barletta M, Gisario A, Rubino G (2011) Scratch response of high-performance thermoset and thermoplastic powders deposited by the electrostatic spray and 'hot dipping'fluidised bed coating methods: the role of the contact condition. Surf Coat Technol 205:5186–5198

Chou L, Marek B, Wagner WR (1999) Effects of hydroxylapatite coating crystallinity on biosolubility, cell attachment efficiency and proliferation in vitro. Biomaterials 20:977–985. https://doi.org/10.1016/S0142-9612(98)00254-3

Costa MI, Verdera D, Vieira MT, Rodrigues DM (2014) Surface enhancement of cold work tool steels by friction stir processing with a pinless tool. Appl Surf Sci 296:214–220. https://doi.org/10.1016/j.apsusc.2014.01.094

Farnoush H, Abdi Bastami A, Sadeghi A, Aghazadeh Mohandesi J, Moztarzadeh F (2013a) Tribological and corrosion behavior of friction stir processed Ti-CaP nanocomposites in simulated body fluid solution. J Mech Behav Biomed Mater 20:90–97. https://doi.org/10.1016/j.jmbbm.2012.12.001

Farnoush H, Sadeghi A, Abdi Bastami A, Moztarzadeh F, Aghazadeh Mohandesi J (2013b) An innovative fabrication of nano-HA coatings on Ti-CaP nanocomposite layer using a combination of friction stir processing and electrophoretic deposition. Ceram Int 39:1477–1483. https://doi.org/10.1016/j.ceramint.2012.07.092

Filiaggi MJ, Coombs NA, Pilliar RM (1991) Student research award in the undergraduate, Master candidate category, or health science degree candidate category, 17th annual meeting of the society for biomaterials, scottsdale, AZ may 1–5, 1991. Characterization of the interface in the plasma-sprayed HA coating/Ti-6Al-4V implant system. J Biomed Mater Res 25:1211–1229. https://doi.org/10.1002/jbm.820251004

Gan YX, Solomon D, Reinbolt M (2010) Friction stir processing of particle reinforced composite. Materials 3:329–350. https://doi.org/10.3390/ma3010329

Ha SW, Mayer J, Koch B, Wintermantel E (1994) Plasma-sprayed hydroxylapatite coating on carbon fibre reinforced thermoplastic composite materials. J Mater Sci Mater Med 5:481–484. https://doi.org/10.1007/BF00058987

Ha SW, Gisep A, Mayer J, Wintermantel E, Gruner H, Wieland M (1997) Topographical characterization and microstructural interface analysis of vacuum-plasma-sprayed titanium and hydroxyapatite coatings on carbon fibre-reinforced poly(etheretherketone). J Mater Sci Mater Med 8:891–896

Hahn B-D et al (2013) Osteoconductive hydroxyapatite coated PEEK for spinal fusion surgery. Appl Surf Sci 283:6–11. https://doi.org/10.1016/j.apsusc.2013.05.073

Huang J, Best S, Bonfield W, Brooks R, Rushton N, Jayasinghe S, Edirisinghe M (2004) In vitro assessment of the biological response to nano-sized hydroxyapatite. J Mater Sci Mater Med 15:441–445

Kokubo T (1998) Apatite formation on surfaces of ceramics, metals and polymers in body environment. Acta Mater 46:2519–2527. https://doi.org/10.1016/S1359-6454(98)80036-0

Kokubo T, Takadama H (2006) How useful is SBF in predicting in vivo bone bioactivity? Biomaterials 27:2907–2915. https://doi.org/10.1016/j.biomaterials.2006.01.017

Landi E, Tampieri A, Celotti G, Sprio S (2000) Densification behaviour and mechanisms of synthetic hydroxyapatites. J Eur Ceram Soc 20:2377–2387. https://doi.org/10.1016/S0955-2219(00)00154-0

Lee JH et al (2013) In vitro and in vivo evaluation of the bioactivity of hydroxyapatite-coated polyetheretherketone biocomposites created by cold spray technology. Acta Biomater 9:6177–6187. https://doi.org/10.1016/j.actbio.2012.11.030

Liu F et al (2009) Micro-scratch study of a magnetron-sputtered Zr-based metallic-glass film. Surf Coat Technol 203:3480–3484

Mendonça G, Mendonça DB, Aragao FJ, Cooper LF (2008) Advancing dental implant surface technology—from micron-to nanotopography. Biomaterials 29:3822–3835

Morishige T, Tsujikawa M, Hino M, Hirata T, Oki S, Higashi K (2008) Microstructural modification of cast Mg alloys by friction stir processing. Int J Cast Met Res 21:109–113. https://doi.org/10.1179/136404608X361774

Müller KH, Motskin M, Philpott AJ, Routh AF, Shanahan CM, Duer MJ, Skepper JN (2014) The effect of particle agglomeration on the formation of a surface-connected compartment induced by hydroxyapatite nanoparticles in human monocyte-derived macrophages. Biomaterials 35:1074–1088. https://doi.org/10.1016/j.biomaterials.2013.10.041

Pan YS, Wang J, Pan CL Research on biological properties of PEEK based composites. In: Applied mechanics and materials, 2013. Trans Tech Publ, pp 3–7

Paoletti A, Lambiase F, Di Ilio A (2016) Analysis of forces and temperatures in friction spot stir welding of thermoplastic polymers. Int J Adv Manuf Technol 83:1395–1407. https://doi.org/10.1007/s00170-015-7669-y

Prasad R, Raghava PM (2012) Fsw of polypropylene reinforced with Al_2O_3 nano composites, effect on mechanical and microstructural properties. Int J Eng Res Appl 2:288–296

Rabiei A, Sandukas S (2013) Processing and evaluation of bioactive coatings on polymeric implants. J Biomed Mater Res Part A 101A:2621–2629. https://doi.org/10.1002/jbm.a.34557

Radin SR, Ducheyne P (1992) Plasma spraying induced changes of calcium phosphate ceramic characteristics and the effect onin vitro stability. J Mater Sci Mater Med 3:33–42. https://doi.org/10.1007/BF00702942

Ratna Sunil B, Sampath Kumar TS, Chakkingal U, Nandakumar V, Doble M (2014a) Friction stir processing of magnesium–nano-hydroxyapatite composites with controlled in vitro degradation behavior. Mater Sci Eng C 39:315–324. https://doi.org/10.1016/j.msec.2014.03.004

Ratna Sunil B, Sampath Kumar TS, Chakkingal U, Nandakumar V, Doble M (2014b) Nano-hydroxyapatite reinforced AZ31 magnesium alloy by friction stir processing: a solid state processing for biodegradable metal matrix composites. J Mater Sci Mater Med 25:975–988. https://doi.org/10.1007/s10856-013-5127-7

Roeder RK, Converse GL, Kane RJ, Yue W (2008) Hydroxyapatite-reinforced polymer biocomposites for synthetic bone substitutes. JOM 60:38–45

Shen X, Bo L, Zhao J, Wei-Zhong X, Sun W (2014) A review of hydroxyapatite microstructure regulation with hydrothermal method. J Funct Mater 45:03006–03010

Shi Z, Huang X, Cai Y, Tang R, Yang D (2009) Size effect of hydroxyapatite nanoparticles on proliferation and apoptosis of osteoblast-like cells. Acta Biomater 5:338–345

Stanford C (2008) Surface modifications of dental implants. Austr Dental J 20:53

Strnad Z, Strnad J, Povysil C, Urban K (2000) Effect of plasma-sprayed hydroxyapatite coating on the osteoconductivity of commercially pure titanium implants. Int J Oral Maxillofac Implants 15:483–490

Wang L, Weng L, Song S, Sun Q (2010) Mechanical properties and microstructure of polyetheretherketone–hydroxyapatite nanocomposite materials. Mater Lett 64:2201–2204

Wang L, Weng L, Song S, Zhang Z, Tian S, Ma R (2011) Characterization of polyetheretherketone–hydroxyapatite nanocomposite materials. Mater Sci Eng A 528:3689–3696

Wang L et al (2014) Polyetheretherketone/nano-fluorohydroxyapatite composite with antimicrobial activity and osseointegration properties. Biomaterials 35:6758–6775

Wu X, Liu X, Wei J, Ma J, Deng F, Wei S (2012) Nano-TiO_2/PEEK bioactive composite as a bone substitute material: in vitro and in vivo studies. Int J Nanomed 7:1215

Xu S, Ma X, Wen H, Tang G, Li C (2014) Effect of annealing on the mechanical and scratch properties of BCN films obtained by magnetron sputtering deposition. Appl Surf Sci

Xue W, Tao S, Liu X, Zheng X, Ding C (2004) In vivo evaluation of plasma sprayed hydroxyapatite coatings having different crystallinity. Biomaterials 25:415–421. https://doi.org/10.1016/S0142-9612(03)00545-3

Zhang G, Leparoux S, Liao H, Coddet C (2006) Microwave sintering of poly-ether-ether-ketone (PEEK) based coatings deposited on metallic substrate. Script Mater 55:621–624. https://doi.org/10.1016/j.scriptamat.2006.06.010